PERGAMON

Vacuum 67 (2002) 185–189

VACUUM
SURFACE ENGINEERING, SURFACE INSTRUMENTATION & VACUUM TECHNOLOGY

www.elsevier.com/locate/vacuum

Effect of microstructures on the coercivity of $Fe_{1-x}B_x$ ($0 \leqslant x \leqslant 0.2$) films prepared by dc magnetron sputtering

Hyoun-Soo Shin[a], Jong-Wook Hong[a], Taesuk Jang[b], Eui-Park Yoon[a], Insoo Kim[c], Geun-Young Yeum[d], Jong-Wan Park[a,*]

[a] *Division of Materials Science and Engineering, Hanyang University, Seoul 133-791, South Korea*
[b] *Division of Metallurgical and Materials Engineering, Sunmoon University, Asan Si, Choongnam 336-708, South Korea*
[c] *Department of Metallurgical Engineering, Dong-A University 840 Hadan-dong, Saha-gu, Busan 604-714, South Korea*
[d] *Department of Materials Engineering, Sungkyunkwan University, Suwon 440-746, South Korea*

Received 9 July 2001; received in revised form 21 September 2001

Abstract

We examined the effects of the variation of boron content in Fe–B films on the microstructure and the coercivity of $Fe_{1-x}B_x$ ($0 \leqslant x \leqslant 0.2$) magnetic thin films by means of transmission electron microscopy, auger electron spectroscopy (AES), field emission scanning electron microscope, atomic force microscopy, and Cu Kα X-ray diffraction pattern analysis. Fe–B thin films were fabricated by dc magnetron sputtering. The sputtered Fe–B films with a boron content <13 at% were found to have metastable Fe(B) solid solution. However, amorphization took place when the boron content was >13 at%. Sputtering pressure was fixed at 1×10^{-3} Torr to prevent oxygen intrusion, which induces a columnar structure in films and eventually deteriorates the soft magnetic properties of the films. Nevertheless, according to the AES depth profile, oxygen and argon atoms were incorporated into all films approximately up to 5 at%. While bare Fe film showed a columnar structure, there was no evidence of columnar structure in boron-containing films. Both root mean square roughness and coercivity decreased drastically with the increase in boron content. These results may be due to the evolution of featureless films with smoother surface by amorphization.

Keywords: Magnetic thin films; Coercivity; Amorphization; Soft magnetic properties

1. Introduction

Recently, magnetostrictive materials have drawn significant interest in sensor and actuator applications. With actuation, the unique non-contact nature makes the magnetostrictive materials particularly attractive for theft detection system or micro-robot application. In most sensor applications, a large magnetostriction needs to be induced at low magnetic field, hence requiring materials that have a combination of large saturation magnetostriction and low saturation field (H_s). Metglas ribbons (Fe-based amorphous alloys) are the best-known candidates for magnetostrictive sensors in a electronic article surveillance system because the amorphous films have low coercivity and high saturation magnetization [1,2]. But at present, these alloys are available only

*Corresponding author. Tel.: +82-2-2290-0386; fax: +82-2-2298-2850.
E-mail address: jwpark@hanyang.ac.kr (J.-W. Park).

PII: S0042-207X(02)00112-4

in the form of thin ribbon ranging from 15 to 50 μm in thickness [3–5]. And a series of post-treatment process such as high-temperature annealing and epoxy treatment are required for the Metglas ribbons to be used as sensors. Therefore, there are many difficulties in micro-sensor application. Consequently, magnetoelastic materials in the form of thin films have to be developed for the miniaturization of sensor. In Fe–B alloy system, researches on the eutectic ($Fe_{83}B_{17}$) and similar composition were extensively conducted by melt spinning, evaporation, and sputtering. However, systematic researches on the variation of microstructures and soft magnetic properties in Fe–B films with boron addition, particularly in the case of small amounts of boron addition, have not been studied well, in spite of the requirement of the thin films for micro-sensor applications.

Therefore, in an effort to develop a material that can be used for micro-sensors, we examined the effect of boron addition on the crystallinity and magnetic properties (especially coercivity) of $Fe_{1-x}B_x$ ($0 \leqslant x \leqslant 0.2$) films in this study.

2. Experimental

Using a standard mechanical-diffusion pump system, $Fe_{1-x}B_x$ ($0 \leqslant x \leqslant 0.2$) thin films were prepared by dc magnetron sputtering with a power of 64 W. Sputtering were performed in 1×10^{-3} Torr argon atmosphere after pumping down to a base pressure of 5×10^{-6} Torr. A microscope cover glass of 130 μm thickness was used as a substrate for better magnetoelastic property. For providing a better condition for amorphous formation, the substrate was cooled by water for high quenching rates and was rotated for homogeneous film composition. The compositions of thin films were controlled by the number of boron pellets (1.27 cm in diameter, 0.25 cm in thickness) which were placed on pure iron target (10.16 cm in diameter, 0.32 cm in thickness). The thickness of the deposited films was measured by using TENCOR ALPHA-STEP 200. Chemical composition of the films was confirmed by auger electron spectroscopy (AES and inductively coupled plasma method. Amorphization of the films was verified by X-ray diffraction (XRD) and transmission electron microscopy (TEM) analysis. root mean square (RMS) roughness and morphology of the films were observed by atomic force microscopy (AFM) and field emission scanning electron microscope (FESEM) (up to 40,000 × magnification), respectively. Magnetic properties of the films were measured by the vibrating sample magnetometer with the maximum applied field of 10 kOe.

3. Results and discussion

In general, a high cooling rate is required for the formation of amorphous phase. In the Fe–B system, however, an alloy of the eutectic composition ($Fe_{83}B_{17}$) can be glassified with minimum cooling rates, while higher cooling rates are required for the composition departure from the eutectic composition.

Fig. 1 shows the variation of the crystallinity of $Fe_{1-x}B_x$ ($0 \leqslant x \leqslant 0.2$) films with the variation of boron addition. Fig. 1(a) is the diffraction pattern of the bare Fe film, revealing the typical pattern of body centered cubic (bcc) α-iron. However, as the

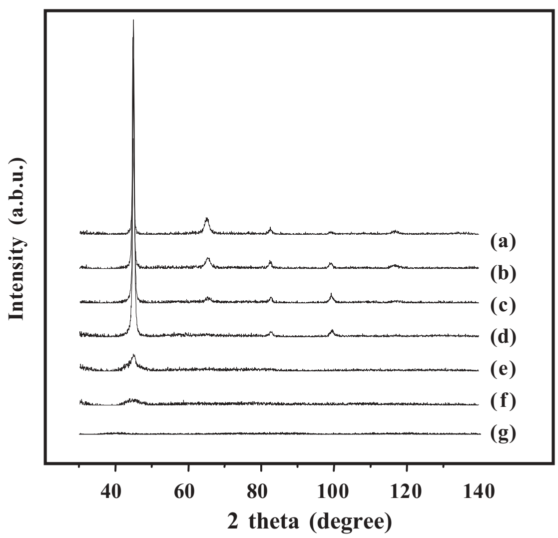

Fig. 1. Cu Kα X-ray diffraction patterns of $Fe_{1-x}B_x$ films: (a) $x = 0$, (b) $x = 0.05$, (c) $x = 0.085$, (d) $x = 0.10$, (e) $x = 0.13$, (f) $x = 0.165$, and (g) $x = 0.20$.

boron content increases (Fig. 1(b)–(d)), the Fe–B films starts to lose the crystallinity and becomes amorphous at 13 at% boron content (Fig. 1(e)). Eventually, the films become totally amorphous when the boron content is >16.5 at% (Fig. 1(f) and (g)).

Fig. 2 exhibits the selective area diffraction (SAD) patterns of the as-deposited Fe–B films. Similar to the XRD patterns in Fig. 1, when the amount of boron addition is relatively small (from Fig. 2(a)–(c)), diffraction lines of bcc α-iron are mainly observed. On the other hand, the film containing 16.5 at% boron shows a hollow pattern at an amorphous phase only. From these results, we confirmed that the films containing <13 at% boron had metastable Fe(B) solid solution with a bcc structure. It has been demonstrated that some amorphous metallic alloys have their local atomic arrangements similar to their crystalline counterparts [6,7]. Considering the XRD patterns in Fig. 1 and SAD patterns in Fig. 2 together, it is concluded that the degree of amorphous formation increases with the increase of boron content, and a fully amorphous film is obtained when the boron content reaches 16.5 at%.

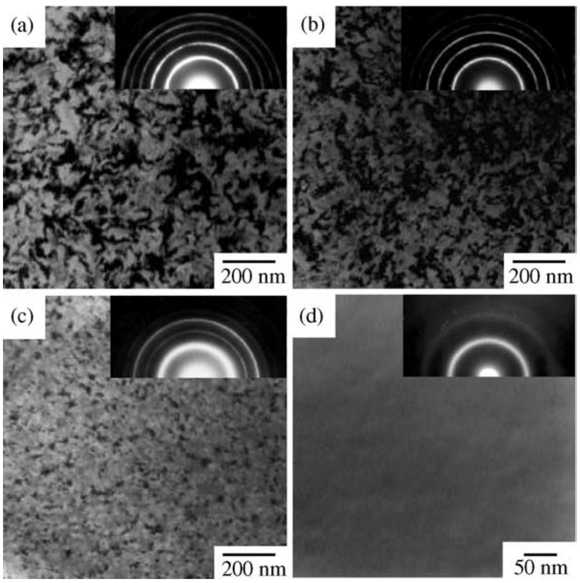

Fig. 2. TEM bright field images and SAD patterns of $Fe_{1-x}B_x$ films: (a) $X=0$, (b) $x=0.05$, (c) $x=0.10$, and (d) $x=0.165$. Average grain size of (a), (b), and (c) is 200, 100, and 10–20 nm, respectively.

Fig. 2 also shows the bright field images of Fe–B films observed by TEM. Fig. 2a is the image of bare Fe film in which the grain size is approximately 200 nm. However, as the boron content increases, the grain size of the films decreases remarkably, eventually resulting in a fully amorphous film. The grain size of the film with 5 at% boron is approximately 100 nm (Fig. 2b), while the film with 10 at% boron has fine grains of 10–20 nm in diameter (Fig. 2c). However, the film of $Fe_{83.5}B_{16.5}$ does not show any appreciable grain up to 40,000 magnifications.

The variation of surface roughness of the films with various boron contents is shown in Fig. 3. The RMS roughness of the bare Fe film is 926 nm, but the roughness of the films decreases almost linearly with the increase of B content. Eventually, $Fe_{80}B_{20}$ film has a very small RMS roughness of 173 nm. AFM images of the Fe–B films had a trend very similar to that of the bright field images in Fig. 2. Therefore, the decrease in RMS roughness of the films is also thought to be due to the amorphization of the films.

In sputter deposition, residual stresses in film experience the transition from a compressive stress (by Ar incorporation) to a tensile stress (by oxygen incorporation) as the sputtering pressure

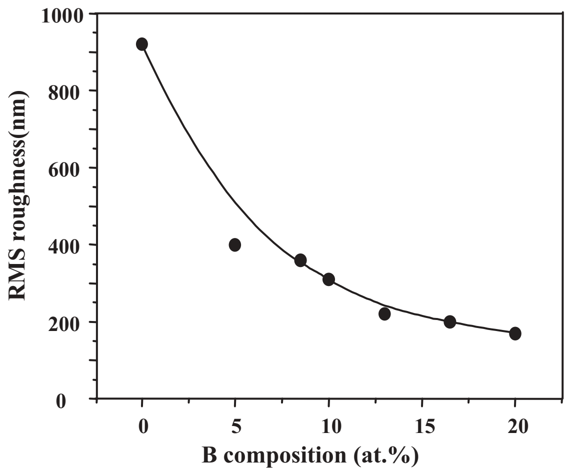

Fig. 3. RMS roughness of $Fe_{1-x}B_x$ films ($0 \leqslant x \leqslant 0.2$).

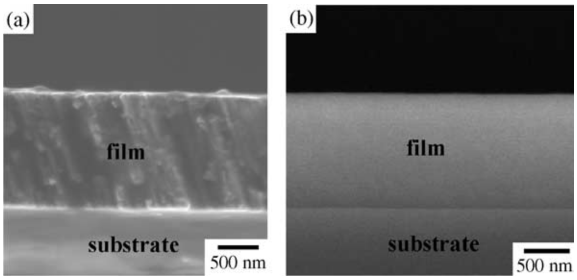

Fig. 4. Cross-sectional FESEM images of (a) Fe, and (b) $Fe_{80}B_{20}$ films.

increases. Particularly, introduction of oxygen in high-sputtering pressure induces a columnar structure in a film, resulting in the deterioration of the soft magnetic properties [9–11]. Due to this reason, as mentioned in the experimental, the sputtering pressure was calibrated at 1×10^{-3} Torr to prevent the formation of columnar structure in the film. Nevertheless, from the results of AES depth profile, it was found that all films had oxygen and argon as impurities approximately 5 at% each. Fig. 4 shows the cross-sectional SEM images of the as-deposited bare Fe and the $Fe_{0.835}B_{0.165}$ films. As can be seen from the figure, the bare Fe film clearly exhibits the columnar structure. However, the columnar structure is not observed any more when boron was added. During deposition, the mobility of atoms depends not only on the substrate temperature but also on the binding energy of the atoms. Then the materials having stronger binding energy are generally considered to have a tendency to form a columnar structure. Impurities, most notably oxygen, have known to reduce the mobility substantially by offering strong binding sites to impinging atoms [12]. Therefore, the diminishing of the columnar structure by the boron addition indicates that the binding energy created by oxygen inclusion is relieved by the addition of boron known as a glassfier.

Changes in the coercivity of the films with boron content are shown in Fig. 5. As shown in the figure, the coercivity of the films decreases remarkably from 54 Oe (in Fe film) to 27.5 Oe (in $Fe_{95}B_5$ film) by adding up to about 5 at% boron.

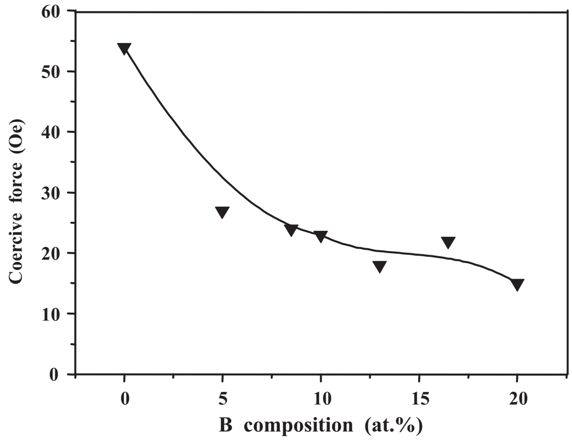

Fig. 5. Coercivity of $Fe_{1-x}B_x$ films ($0 \leqslant x \leqslant 0.2$).

Then, it decreases gradually as the boron content increases further, yielding the smallest coercivity of 15.1 Oe in the case of the $Fe_{80}B_{20}$ film. Although the expected coercivity of the ribbon-type materials for sensor application is about 10 Oe [13] and it is presumed that the coercivity values suitable for thin film sensors are not far from this value, it is not yet clear as to what coercivity values are desirable for thin film sensors. The coercivity of a film is generally known to depend on various factors such as grain size, internal and external stresses, impurities (argon, oxygen, or target impurities), sputtering pressure, surface roughness, induced anisotropy, composition, magnetostriction, pressure–distance product, and thickness of the film [9,14,15]. However, an amorphous alloy usually has low coercivity because it has a homogeneous body that contains almost no grain boundary or structural defects of any noticeable size. Therefore, the decrease of coercivity with the increase of boron addition is attributed to the amorphization of the films by the boron addition, which forms a film with a featureless structure and a smooth surface.

4. Conclusions

In $Fe_{1-x}B_x$ ($0 \leqslant x \leqslant 0.2$) films prepared by dc magnetron sputtering, microstructures and coercivities of the films were changed drastically with increasing boron content. The films with <13 at% boron had metastable Fe(B) solid solution of BCC structure. However, the film became amorphous with the addition of 13 at% B, and a complete amorphous film was attained at 16.5 at% B. RMS roughness of the films also decreased largely due to the amorphization. It was found that, from the AES analysis, all films had impurities such as oxygen and argon approximately up to 5 at%. However, the columnar structure was not observed in the films containing certain amounts of boron in the films. It implies that the increase in the boron addition further surpasses the mobility of atoms resulting in the formation of amorphous phase. The coercivity of the films decreased remarkably, from 54 to 27.5 Oe, when only 5 at% of boron was incorporated into the films. Then it decreased gradually as the boron addition increased, yielding a small coercivity of 15.1 Oe for the $Fe_{80}B_{20}$ film. The decrease of the coercivity is attributed to the amorphization of the films by the boron addition, which makes a film with small noticeable defects and surface roughness.

Acknowledgements

The authors gratefully acknowledge the financial support of the Korea Science and Engineering Foundation [KOSEF 97-0300-1101-5].

References

[1] Fukuda T, Hosokai H, Ohyama H, Hashimoto H, Arai F. IEEE MEMS'91 1991;210.
[2] Kim CK. Mater Sci Eng B 1995;34:1.
[3] Kersey AD. J Lightwave Technol 1985;LT-3:1.
[4] Freestone J. J Appl Phys 1991;70:6531.
[5] Vincent JH. GEC J Res 1993;10:179.
[6] Minoru T, Masami K. Jpn J Appl Phys 1981;20(10):1821.
[7] Hasegawa R, Ranjan R. J Appl Phys 1978;49:4174.
[9] Mattingley AD, Shearwood C, Gibbs MRJ. IEEE Trans Mag 1994;30:4806.
[10] Hudson C, Somekh RE. Mater Res Soc Symp Proc 1992;239:145.
[11] Shimada Y, Kojima H. J Appl Phys Sci Instrum 1988;21:1167.
[12] Leamy HJ, Dirks AG. J Appl Phys 1978;49(6):3430.
[13] Giselher H. US Patent No.5841348, 1998.
[14] Materne A, Morieceau H, Blanchard B, Floreston J. IEEE Trans Mag 1988;24:1752.
[15] Harris VG, Oliver SS, Nowak WB. J Vac Sci Technol 1990;A8(3):1325.